Functional Na^+ Channels in Cell Adhesion probed by Transistor Recording

Markus Schmidtner and Peter Fromherz
Department of Membrane and Neurophysics, Max Planck Institute for Biochemistry, Martinsried/Munich, Germany

ABSTRACT Cell membranes in a tissue are in close contact to each other, embedded in the extracellular matrix. Standard electrophysiological methods are not able to characterize ion channels under these conditions. Here we consider the area of cell adhesion on a solid substrate as a model system. We used HEK 293 cells cultured on fibronectin and studied the activation of $Na_V1.4$ sodium channels in the adherent membrane with field-effect transistors in a silicon substrate. Under voltage clamp, we compared the transistor response with the whole-cell current. We observed that the extracellular voltage in the cell-chip contact was proportional to the total membrane current. The relation was calibrated by alternating-current stimulation. We found that Na^+ channels are present in the area of cell adhesion on fibronectin with a functionality and a density that is indistinguishable from the free membrane. The experiment provides a basis for studying selective accumulation and depletion of ion channels in cell adhesion and also for a development of cell-based biosensoric devices and neuroelectronic systems.

INTRODUCTION

This article deals with the coupling of the ion current of Na^+ channels in a mammalian cell to the electron current of transistors in a silicon chip. The issue is related with two fields of biophysical research, the electrical characterization of cell membranes in contact with the extracellular matrix and the development of bioelectronic devices for biosensorics and neuroelectronics.

We consider a system that consists of $Na_V1.4$ channels in HEK 293 cells on an electrolyte/oxide/silicon transistor. A schematic cross section is shown in Fig. 1 *a* and a micrograph is depicted in Fig. 1 *b*. Cell membrane and silicon dioxide are separated by a thin film of electrolyte that plays the role of a gate for a field-effect transistor with source and drain. The cell is joined to a micropipette to control the intracellular voltage and to measure the current through the cell membrane. Voltage-gated Na^+ channels are opened by a depolarizing intracellular voltage. Ion current through the adherent membrane flows along the thin film of electrolyte and gives rise to an extracellular voltage between cell and chip that modulates the source-drain current. With a seal resistance of the cell-chip junction, that is determined in an alternating-current (AC) experiment, we can evaluate the ion current through the adherent membrane and compare it with the total membrane current.

A similar approach was used for potassium channels in cultured neurons (1) and with recombinant hSlo and Kv1.3 potassium channels in HEK 293 cells (2,3). There are three reasons to extend the study to recombinant Na^+ channels: i), The function of Na^+ channels is crucial for cell-cell contacts in neuronal tissue and for cell-surface contacts in neuronal interfacing. ii), The chemical interaction of Na^+ ions with the gate oxide of transistors is weak (3). A simple ohmic relation is expected between the measured extracellular voltage and the ion current through the attached membrane without complications that arise from ion binding to the oxide, as in the case of potassium (3). iii), The ion specificity of Na^+ channels is similar to that of many ligand-gated ion channels such that their interfacing to transistors is a basis for the development of cellular biosensors.

After a description of the methods, we summarize the one-compartment model of cell-transistor junctions that is used for an interpretation of the data. Then the cell-chip interaction is described for a selected HEK 293 cell as achieved by AC stimulation with a capacitive cell-transistor coupling and by direct-current (DC) depolarization with a coupling mediated by Na^+ current. Finally, the variability of the AC and DC data for a set of cells that is due to cell shape, channel distribution, and cell-transistor geometry is discussed.

MATERIALS AND METHODS

Cells

HEK 293 cells (DSMZ, Braunschweig, Germany) were transfected (calcium phosphate method) with the mammalian expression vector pcDNA3.1(+) (Invitrogen, Karlsruhe, Germany) coding for the α-subunit of the $Na_V1.4$ channel from rat skeletal muscle (4,5). Stably transfected clones were obtained after 2 months of selection by cultivating in 5% CO_2 at 37°C on 35-mm plastic dishes (Falcon, Becton Dickinson, Plymouth, UK) in a 1:1 mixture of Dulbecco's modified Eagle's medium and F-12 nutrient mixture containing Glutamax-I (No. 31331, Invitrogen) supplemented with 10% (vol/vol) heat inactivated bovine serum (Invitrogen) and 200 μg/ml geneticin (G418 disulfate salt, Sigma, Deisenhofen, Germany). The stably transfected cells were cultured in the same medium with 100 μg/ml geneticin. They were split at 70–80% confluency and diluted with Dulbecco's modified Eagle's medium without geneticin at a ratio 1:50. The experiments were started 1 day after replating the cells on the chips. Tetrodotoxin (Sigma) at

Submitted June 9, 2005, and accepted for publication September 27, 2005.

Address reprint requests to Peter Fromherz, Dept. of Membrane and Neurophysics, Max Planck Institute for Biochemistry, Martinsried/Munich, Germany 82152. E-mail: fromherz@biochem.mpg.de.

0006-3495/06/01/183/07 $2.00

doi: 10.1529/biophysj.105.068361

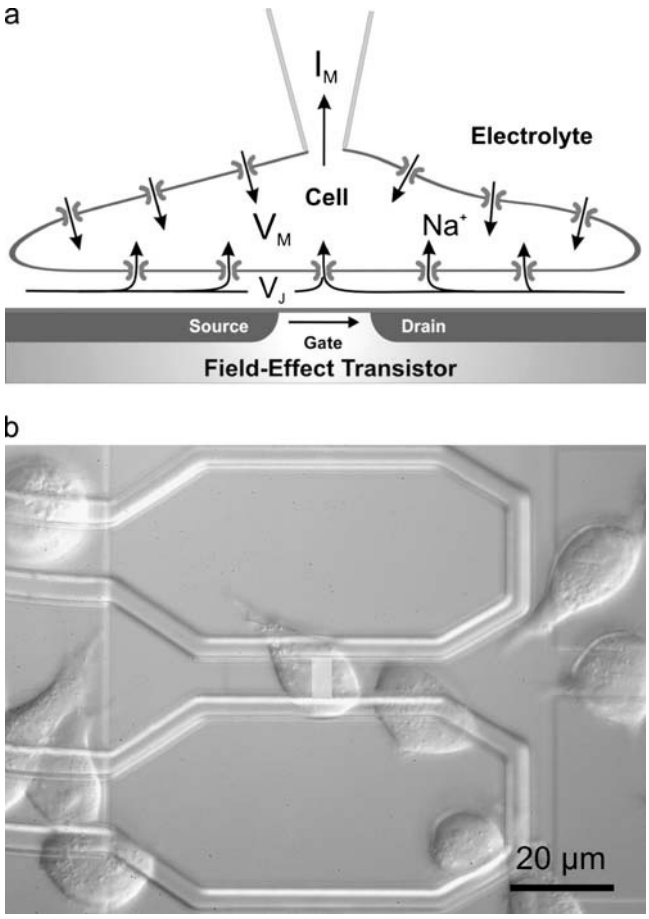

FIGURE 1 Cell-transistor system. (*a*) Schematic cross section. (not to scale: diameter of cell, ~20 μm, distance of cell and chip, ~70 nm). The intracellular voltage V_M is controlled by a patch-clamp pipette. The total membrane current I_M arises from the attached and free parts of the membrane. The extracellular voltage V_J in the cell-chip junction arises from current through the attached membrane that flows along the resistance of the cell-chip junction. It modulates the source-drain current of the transistor. (*b*) Differential interference contrast micrograph of HEK 293 cells on a silicon chip with a transistor. The gate beneath a cell is visible as a bright rectangle in the center, with drain and source at left and right, respectively. The octagonal structures above and below are capacitors that are not used in the experiments.

a concentration of 150 nM was applied for selective blocking of Na^+ channels.

Chips

We used silicon chips with linear arrays of p-type electrolyte/oxide/silicon field-effect transistors (6). The size of the metal-free gates is 3×8 μm. The transistors are insulated from each other by local oxidation of silicon. The gate oxide with a thickness of 10 nm is fabricated by rapid thermal processing at 1000°C. We bonded the chips to a ceramic package (CPGA 208L, Spectrum, San Jose, CA) and attached a perspex chamber for the culture medium. After each use, the chips were wiped with 2% (v/v) detergent (Tickopur RP100, Bandelin, Berlin, Germany), rinsed with milli-Q water (Millipore, Bedford, MA), and dried. The surface was made hydrophobic by exposure to hexamethyldisilazane vapor (30 min), sterilized with ultraviolet light, coated with fibronectin (Sigma) (15 μg/ml in phosphate-buffered saline (5 h), and rinsed with phosphate-buffered saline.

Setup

A cell suspension (1 ml) was seeded on a silicon chip with transistors. We replaced the culture medium by an extracellular electrolyte with a reduced concentration of NaCl with (in mM) 50 NaCl, 2 KCl, 1.5 $CaCl_2$, 1 $MgCl_2$, 10 HEPES, and 205 glucose. We adjusted it to pH 7.4 with NaOH and to an osmolality of 330 mOsm/kg with glucose (all chemicals from Sigma). The resistivity was $\rho_E = 167\Omega$cm. Micropipettes were pulled from borosilicate glass (Science Products, Hofheim, Germany), fire polished, and coated with Sylgard (Dow Corning, Midland, MI). They were filled by an intracellular solution with (in mM) 12 NaCl, 100 CsF, 28 CsCl, 10 EGTA, and 10 HEPES. A pH of 7.4 was adjusted with KOH and an osmolality of 330 mOsm/kg with glucose. The Na^+ reversal voltage was 36.5 mV. A patch-clamp amplifier (Axopatch 200B, Axoclamp, Union City, CA) was connected to the pipette and to a Ag/AgCl electrode (WPI, Sarasota, FL) in the bath at ground potential. Cells were selected with a microscope (Axioskop 2 FS, Zeiss, Oberkochen, Germany).

In a linear range around a working point, the source-drain current I_D is described by Eq. 1 with a transconductance $(\partial I_D/\partial V_{ESi})_{VSD}$ and a constant V^0_{ESi} that depends on the threshold of the transistor:

$$I_D = \left(\frac{\partial I_D}{\partial V_{ESi}}\right)_{V_{SD}} (V_{ESi} - V^0_{ESi}). \quad (1)$$

We applied a bias voltage of $V_{ESi} = -3.0$ V between the Ag/AgCl electrode in the bath and bulk silicon and a voltage $V_{SD} = 2.9$ V between source and drain, with the source connected to bulk silicon. The source-drain current was around $I_D = 100$ μA. Before each experiment, the transistors were calibrated by modulating the bath voltage. The transconductance was around -100 nA/mV.

Calibration

Cell-chip coupling is described by the transfer of intracellular voltage V_M to the extracellular voltage V_J in the cell-chip junction in comparison to the total membrane current I_M. For DC measurements, intracellular voltage and membrane current were directly obtained from the patch-clamp amplifier using its compensation facilities. The extracellular voltage was obtained from the change ΔI_D of the source-drain current that was induced by cell stimulation. At a bias voltage V_{ESi}, the current change was expressed in terms of a voltage shift ΔV_{FET} of the transistor characteristics according to Eq. 2 and that shift was identified with an extracellular voltage V_J according to Eq. 3:

$$\Delta V_{FET} = \Delta I_D \left(\frac{\partial I_D}{\partial V_{ESi}}\right)^{-1}_{VSD} \quad (2)$$

$$V_J = \Delta V_{FET}. \quad (3)$$

AC measurements were performed to determine the membrane capacitance and the conductance of the cell-chip contact. We determined the modulation of membrane current $\underline{I}_M$ and extracellular voltage $\underline{V}_J$ as induced by an alternating intracellular voltage $\underline{V}_M$ of angular frequency ω. $\underline{V}_J$ was computed from the modulation $\underline{I}_D$ of the source-drain current according to Eqs. 2 and 3. To determine $\underline{V}_M$ and $\underline{I}_M$, we did not use the full compensation facilities of the amplifier. Instead, we measured access resistance R_A, leak resistance R_L, and stray capacitance C_{ST} of the pipette and computed $\underline{V}_M$ and $\underline{I}_M$ from the applied voltage $\underline{V}_P$ and the measured current $\underline{I}_P$, according to Eqs. 4 and 5, which are derived from the circuit of Fig. 2:

$$\underline{V}_M = (1 + i\omega R_A C_{ST})\underline{V}_P - R_A \underline{I}_P \quad (4)$$

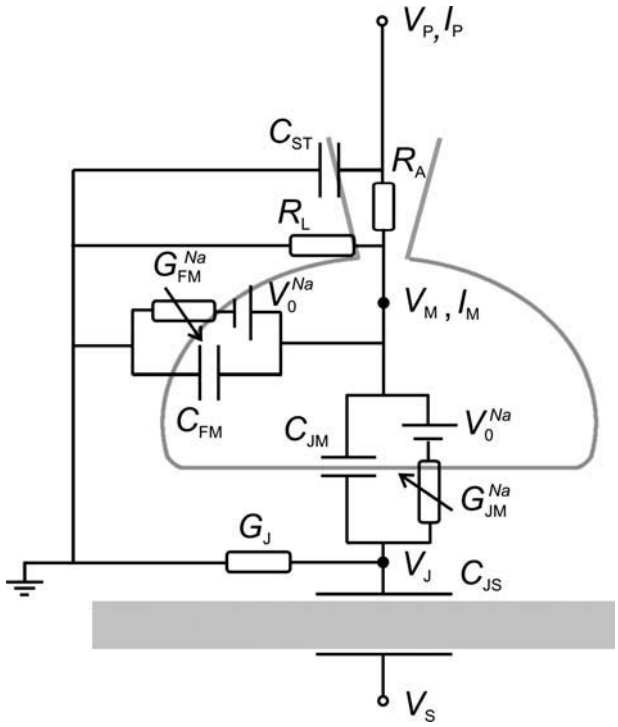

FIGURE 2 Electrical circuit of cell-chip system. A voltage V_P is applied to the pipette and a current I_P is measured through the pipette with access resistance R_A, leak resistance R_L, and stray capacitance C_{ST}. The voltage in the cell and the current through the cell membrane are V_M and I_M. V_0^{Na} is the Na^+ reversal voltage. The core-coat conductor of the cell-chip junction with area A_J is described by a one-compartment model with capacitance $C_{JM} = A_J c_M$ and Na^+ conductance $G_{JM}^{Na} = A_J g_{JM}^{Na}$ of the attached membrane, a capacitance $C_{JS} = A_J c_S$ of the substrate, a seal conductance $G_J = A_J g_J$, and an extracellular voltage V_J in the junction. With a total membrane area A_M, the free membrane is described by a capacitance $C_{FM} = (A_M - A_J)c_M$ and Na^+ conductance $G_{FM}^{Na} = (A_M - A_J)g_{FM}^{Na}$. $c_M, c_S, g_{JM}^{Na}, g_{FM}^{Na}$ and g_J are area-specific parameters.

$$\underline{I}_M = \left(1 + \frac{R_A}{R_L}\right)\underline{I}_P - \frac{1}{R_L}[1 + i\omega(R_A + R_L)C_{ST}]\underline{V}_P. \quad (5)$$

The stray capacitance C_{ST} of the pipette was measured in a cell-attached configuration and compensated with the amplifier. After breakthrough of the membrane, a holding voltage of −90 mV was applied. Without changing the compensation, an alternating voltage $\underline{V}_P$ was superposed in a frequency range $f = 5\,\text{Hz} - 10\,\text{kHz}$ with an amplitude of 4 mV. Amplitude and phase of the pipette current $\underline{I}_P$ were measured with a lock-in amplifier (SR 850, Stanford Research Systems, Sunnyvale, CA). The spectrum of the admittance $Y_P = \underline{I}_P/\underline{V}_P$ was evaluated with the circuit of Fig. 2 using Eq. 6 with $C_{ST} = 0$ due to compensation. As a result, we obtained R_A and R_L at an admittance Y_M of the cell:

$$Y_P = \frac{R_L^{-1} + Y_M}{R_A(R_L^{-1} + Y_M) + 1} + i\omega C_{ST}. \quad (6)$$

Protocol

All experiments were performed at ambient temperature. At first we determined stray capacitance, access resistance, and seal resistance as described above. We accepted leak resistances down to $R_L = 500\,M\Omega$ to attain a sufficiently large number of measurements with cells on transistors. Then we characterized the strength of cell-chip coupling by an AC measurement at a holding voltage $V_M = -90\,\text{mV}$. We applied an alternating voltage $\underline{V}_P$ to the pipette and measured amplitude and phase for the pipette current $\underline{I}_P$ and for the modulation $\underline{I}_D$ of the source-drain current with two lock-in amplifiers. The intracellular voltage $\underline{V}_M$ and the membrane current $\underline{I}_M$ were computed with Eqs. 4 and 5. The extracellular voltage $\underline{V}_J$ was obtained from the modulated transistor signal with Eqs. 2 and 3. The amplitude of the stimulation voltage was 10 mV to attain a sufficient transistor signal. The frequency was limited to $f = 200$–1500 Hz. At lower frequencies, the transistor record was too small, at higher frequencies nonlinear features of the cell-chip coupling appeared.

For the DC experiments, we used the full compensation facility of the amplifier to eliminate stray and membrane capacitance, leak resistance, and access resistance. Starting from a holding potential of $V_M = -120\,\text{mV}$, we applied rectangular voltage pulses of 10-ms duration from $V_M = -70\,\text{mV}$ to $+35\,\text{mV}$ with a P/4 protocol to eliminate capacitive transients. We measured the membrane current I_M and the change of source-drain current at 15 depolarizing voltages V_M. The extracellular voltage V_J was evaluated with Eqs. 2 and 3. For each voltage, 20 measurements were averaged to improve the signal/noise ratio of the transístor signals. The data were filtered at 10 kHz and sampled at 30 kHz.

RESULTS AND DISCUSSION

At first we summarize the one-compartment model of a cell-transistor junction that is used to evaluate the data. Then the results of a selected cell-chip system are described for AC and DC stimulation (Figs. 3–5). Finally, for a set of cells the variability of coupling is considered as caused by cell shape, channel distribution, and cell-transistor geometry (Figs. 6 and 7).

One-compartment model

A cell-chip junction is a planar core-coat conductor with a sheet of electrolyte between cell membrane and chip oxide (7,8). Capacitive and ionic currents flow through the adherent membrane and along the sheet resistance $r_J = \rho_J/d_J$ that is determined by the width d_J and resistivity ρ_J of the electrolyte. As a result, a profile of extracellular voltage is created in the cell-chip junction (see Appendix). Here, we use a one-compartment model with a representative extracellular voltage V_J as represented by the equivalent circuit of Fig. 2 (see Appendix) (7,9). In an approximation for small signals with $|V_J| \ll |V_M - V_0^{Na}|$ and $|dV_J/dt| \ll |dV_M/dt|$, where V_M is the intracellular voltage and V_0^{Na} is the Na^+reversal voltage, V_J is determined by the current balance in the cell-chip junction of area A_J according to Eq. 7. The concomitant current I_M through the total membrane of area A_M is given by Eq. 8. The relations are expressed in terms of area-specific parameters, the membrane capacitance c_M, the Na^+ conductances g_{JM}^{Na} and g_M^{Na} of attached and average membrane, and the conductance g_J of the cell-transistor junction:

$$A_J g_J V_J \approx A_J c_M \frac{dV_M}{dt} + A_J g_{JM}^{Na}(V_M - V_0^{Na}) \quad (7)$$

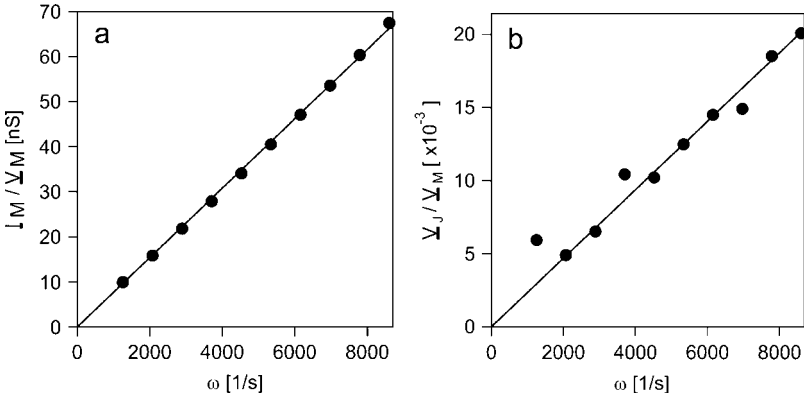

FIGURE 3 AC measurement of cell-transistor system at an intracellular holding voltage of −90 mV. (*a*) Amplitude of membrane admittance $\underline{I}_M/\underline{V}_M$ versus angular frequency ω. The fitted line has a slope of 7.8 ± 0.08 pF. (*b*) Amplitude of voltage transfer $\underline{V}_J/\underline{V}_M$ versus angular frequency ω. The fitted line has a slope of 2.4 ± 0.08 μs.

$$I_M \approx A_M c_M \frac{dV_M}{dt} + A_M g_M^{Na}(V_M - V_0^{Na}). \quad (8)$$

The area-specific conductance g_J of the junction depends on the sheet resistance r_J of the core-coat conductor according to Eq. 9. A geometry parameter η_J accounts for the position of transistor recording and the shape of the adhesion area (see Appendix) (7). It is $\eta_J = 4\pi$ for local recording in the center of a compact circular junction and larger for a more peripheral recording and for a less compact area of adhesion:

$$\frac{1}{g_J} = \frac{A_J r_J}{\eta_J}. \quad (9)$$

AC experiment

We selected a transfected HEK 293 cell on a transistor and connected it to a patch pipette. From an admittance measurement we obtained an access resistance $R_A = 3.5\,M\Omega$ and a leak resistance $R_L = 530\,M\Omega$. The cell was held at a bias voltage $V_M = -90$ mV, where the Na^+ channels are closed. We applied an alternating voltage to the pipette. The alternating voltage $\underline{V}_M$ in the cell and the alternating membrane current $\underline{I}_M$ were evaluated from the pipette signal, and the alternating voltage $\underline{V}_J$ in the junction was determined with the transistor, as described in the Methods section. The amplitudes of membrane admittance $\underline{I}_M/\underline{V}_M$ and of voltage transfer $\underline{V}_J/\underline{V}_M$ are plotted in Fig. 3, *a* and *b*. Both linearly increase with the angular frequency ω.

When we stimulate a cell without ion conductances by alternating voltage $\underline{V}_M$, the one-compartment model yields Eq. 10 for the alternating extracellular voltage $\underline{V}_J$ and Eq. 11 for the alternating membrane current $\underline{I}_M$:

$$\underline{V}_J \approx \frac{i\omega c_M}{g_J}\underline{V}_M \quad (10)$$

$$\underline{I}_M \approx i\omega A_M c_M \underline{V}_M. \quad (11)$$

Using these relations for a linear fit of the data in Fig. 3, we obtain a time constant $c_M/g_J = 2.4 \pm 0.1$ μs and a membrane capacitance $A_M c_M = 7.8 \pm 0.1$ pF. With $c_M = 1\,\mu F/cm^2$, the area specific conductance of the cell-transistor junction is $g_J = 420\,mS/cm^2$ and the total membrane area is $A_M = 780\,\mu m^2$. From a micrograph of the cell, we estimated an area of cell adhesion $A_J = 200\,\mu m^2$. We obtained a fraction of the attached membrane $\alpha_{JM} = A_J/A_M = 0.26$ and a global conductance of the cell-chip junction $G_J = A_J g_J = 0.84\,\mu S$.

Obviously, the one-compartment model, with Eqs. 10 and 11, implies that the extracellular voltage $\underline{V}_J$ and the membrane current $\underline{I}_M$ are proportional to each other when the AC membrane conductance is varied by the frequency according to Eq. 12:

$$\underline{V}_J = \frac{1}{g_J A_M}\underline{I}_M. \quad (12)$$

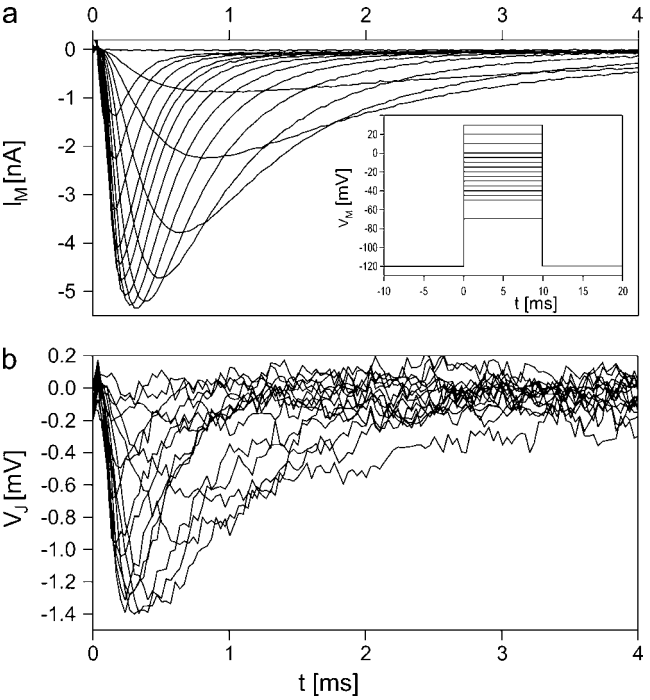

FIGURE 4 DC coupling of Na^+ channels to transistor. (*a*) Membrane current $I_M(t)$ versus time for 15 different voltage pulses with a duration of 10 ms starting from a holding voltage of −120 mV (*inset*). (*b*) Extracellular voltage in the cell-chip junction $V_J(t)$ versus time. Twenty signals are averaged for $I_M(t)$ and $V_J(t)$ at each membrane voltage.

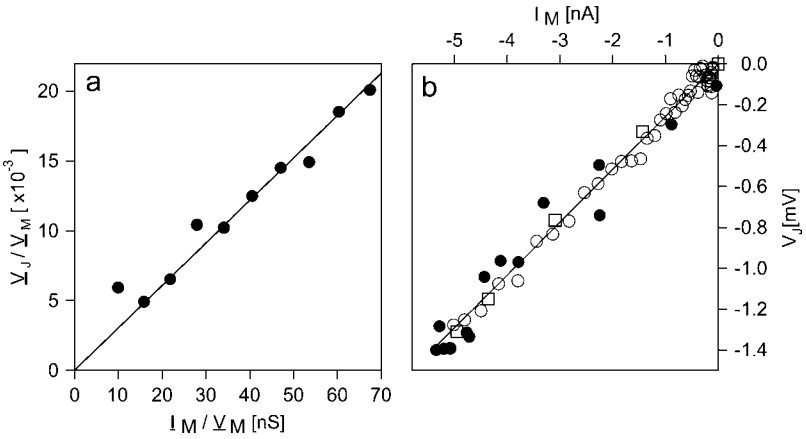

FIGURE 5 Transimpedance of cell-chip system for AC and DC stimulation. (*a*) Voltage transfer $\underline{V}_J/\underline{V}_M$ versus membrane admittance $\underline{I}_M/\underline{V}_M$ for AC stimulation at an intracellular holding voltage $V_M = -90\,mV$. The slope of the fitted line indicates an AC transimpedance of $\underline{V}_J/\underline{I}_M = 308\,k\Omega$. (*b*) Extracellular voltage $V_J(t)$ versus membrane current $I_M(t)$ at an intracellular voltage $V_M = -20\,mV$(data at intervals of 0.033 ms; □, downstroke; ○, upstroke), and minimum extracellular voltages V_J versus minimum membrane currents I_M for 15 depolarizations (●). The slope of the fitted line indicates a DC transmimpedance of $V_J/I_M = 260\,k\Omega$.

We replotted the data of Fig. 3, *a* and *b*, as $\underline{V}_M$ versus $\underline{I}_M$ in Fig. 5 *a*. The slope of the linear relation represents an ''AC transimpedance'' of $\underline{V}_J/\underline{I}_M = 308\,k\Omega$. This crucial electrophysiological parameter of a cell-transistor system is a product of the global resistance of the junction $G_J^{-1} = 1.2\,M\Omega$ and the fraction of attached membrane $\alpha_{JM} = 0.26$.

DC experiment

After completing the AC measurements, we held the cell at an intracellular voltage of $-120\,mV$. While compensating the effects of access resistance and capacitances, we applied 15 rectangular voltage pulses V_M of 10-ms duration to the cell and recorded the membrane current I_M and the extracellular voltage V_J as a function of time. To attain a sufficient signal/noise ratio of the transistor response, we averaged twenty records of the transistor signal and also of the membrane current at each voltage. The results are plotted in Fig. 4, *a* and *b*. The membrane inward current increased within a few hundred microseconds after depolarization and decayed within 2 ms. The maximum current increased and decreased with enhanced depolarization. These features are typical for Na^+ channels with their voltage-dependent activation and inactivation. The response of the transistor showed a transient negative extracellular voltage with increasing and decreasing amplitude for larger intracellular depolarizations. The waveforms of the membrane current and of the transistor signal were similar. Addition of tetrodotoxin completely suppressed the membrane current as well as the transistor signal (data not shown). We conclude that the transistor signal is caused by Na^+ current.

According to the one-compartment model, the extracellular DC voltage V_J in the cell-transistor junction is determined by the Na^+ conductance g_{JM}^{Na} in the attached membrane according to Eq. 13 and the membrane current is given by Eq. 14 with an area specific Na^+ conductance g_M^{Na} of the total cell membrane:

$$V_J \approx \frac{g_{JM}^{Na}}{g_J}(V_M - V_0^{Na}) \tag{13}$$

$$I_M \approx A_M g_M^{Na}(V_M - V_0^{Na}). \tag{14}$$

The dynamics of Na^+ channels is usually described as a product $g^{Na}(t) = \bar{g}^{Na}p^{Na}(t)$ of a maximum conductance $\bar{g}^{Na}$ and a probability $p^{Na}(t)$ for the channels to be in their open state. If the channel dynamics in the attached cell membrane and in the average cell membrane is identical with $p_{JM}^{Na}(t) \equiv p_M^{Na}(t)$, we expect that the extracellular voltage $V_J(t)$ and the membrane current $I_M(t)$ are proportional to each other. We obtain Eq. 15, where $\bar{g}_{JM}^{Na}$ and $\bar{g}_M^{Na}$ are the maximum Na conductances in the attached and average membrane:

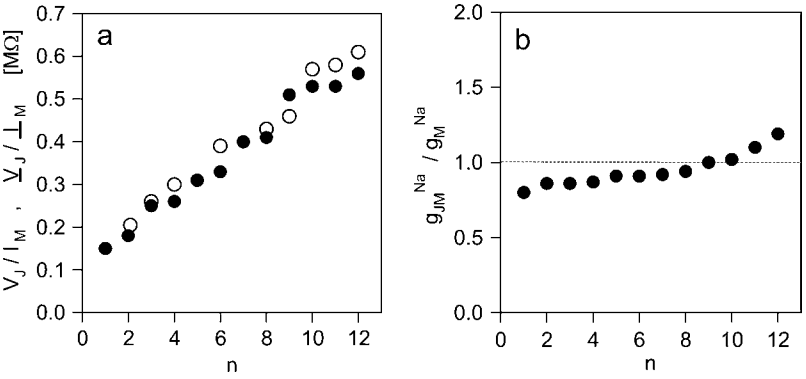

FIGURE 6 Transimpedance and channel distribution of 12 cell-transistor systems. (*a*) DC transimpedance V_J/I_M (●) and AC transimpedance $\underline{V}_J/\underline{I}_M$ (○) in the same order of increasing values. (*b*) Quotient of DC and AC impedance indicating the ratio $\bar{g}_{JM}^{Na}/\bar{g}_M^{Na}$ of the maximum area-specific sodium conductance in attached and average membrane in the order of increasing values. The ratio $\bar{g}_{JM}^{Na}/\bar{g}_M^{Na} = 1$ is marked by a dotted line.

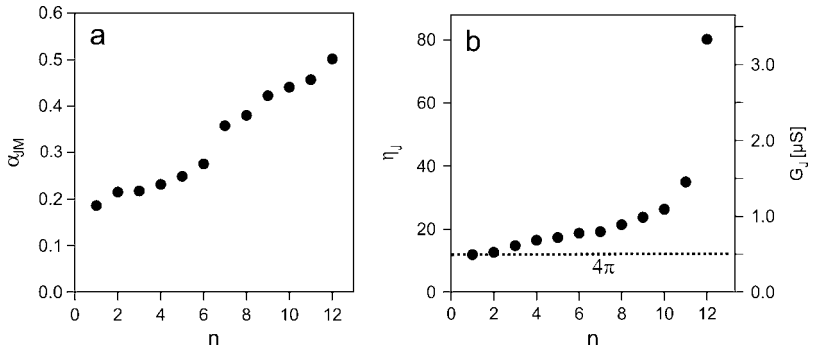

FIGURE 7 Cell-shape parameter and geometry parameter of 12 cell-transistor systems. (*a*) Ratio of attached and total membrane area $\alpha_{JM} = A_J/A_M$ in the order of increasing values. (*b*) Global seal conductance G_J (*right scale*) and geometry parameter η_J (*left scale*) for a sheet resistance $r_J = 24\,M\Omega$ in the order of increasing values. $\eta_J = 4\pi$ is marked as a dotted line.

$$V_J = \frac{1}{g_J A_M}\frac{\bar{g}_{JM}^{Na}}{\bar{g}_M^{Na}} I_M. \tag{15}$$

We replotted the data of the time-dependent extracellular voltage $V_J(t)$ versus the time-dependent membrane current $I_M(t)$ in Fig. 5 *b* for an intracellular voltage $V_M = -20\,mV$. In addition, we plotted the minima of the voltage V_J versus the minima of the current I_M for all time-dependent signals. We found a linear relation between V_J and I_M for both sets of data. We conclude that the functionality of voltage-dependent dynamics is the same for the Na^+ channels in the area of cell adhesion and in the free membrane. The slope of the fitted line in Fig. 5 *b* indicates a ''DC transimpedance'' of $V_J/I_M = 260\,k\Omega$ of the cell-transistor junction. It is lower than the AC transimpedance $\underline{V}_J/\underline{I}_M = 308\,\Omega$. Comparing Eqs. 12 and 15, that difference can be assigned to a changed density of Na^+ channels in the area of adhesion with a ratio of the area-specific conductances $\bar{g}_{JM}^{Na}/\bar{g}_M^{Na} = 0.75$.

Statistics of Na channel distribution

The yield of good cell-transistor couplings was modest. We were faced with three specific effects: i), The probability for a cell to properly cover a transistor was fairly low. Usually only 1–2 cells could be used on a chip. ii), Due to the transistor noise, a whole-cell Na^+ current above 2 nÅ was required to obtain a sufficient signal/noise ratio. Only ~10% of the cells on a transistor were suitable. iii), Data acquisition for the AC measurements at different frequencies and for the repetitive DC measurements at different voltages required a stable cell-chip contact and a stable seal resistance of the pipette for at least 10 min.

We recorded a complete set of AC and DC measurements for 12 cell-transistor systems. The AC and DC transimpedances $\underline{V}_J/\underline{I}_M$ and V_J/I_M are plotted in the same order in Fig. 6 *a*. Apparently, the variability of both parameters is rather similar between 150 and 600 kΩ without a characteristic plateau at an average value.

The result suggests that the variability of the DC transimpedance is determined by the same parameters as the variability of the AC transimpedance. Considering Eqs. 13 and 14, the DC transimpedance can be written as a product of the AC transimpedance and the ratio $\bar{g}_{JM}^{Na}/\bar{g}_M^{Na}$ of area-specific Na^+ conductances in the attached and average membrane according to Eq. 16:

$$\frac{V_J}{I_M} = \frac{\underline{V}_J}{\underline{I}_M}\frac{\bar{g}_{JM}^{Na}}{\bar{g}_M^{Na}}. \tag{16}$$

We eliminated the variability in the DC transimpedance that is present in the AC transimpedance by dividing the two parameters for each cell. As a result we obtained the ratios $\bar{g}_{JM}^{Na}/\bar{g}_M^{Na}$ of Na^+ conductances that are plotted in Fig. 6 *b* in an order of increasing values. The distribution is rather narrow, centered around a plateau of $\bar{g}_{JM}^{Na}/\bar{g}_M^{Na} = 0.9$ with a Gaussian spread of $\sigma = 0.1$. We conclude i), that there is no significant depletion or accumulation of Na channels in the area of adhesion; and ii), the cell membrane in the area of adhesion is rather well defined with respect to channel expression.

Statistics of cell-chip junction

Finally, we consider the variability of cell-transistor coupling as revealed by the AC transimpedance. Using Eqs. 9 and 12, we write the AC transimpedance in terms of the global conductance $G_J = \eta_J/r_J$ of the cell-transistor junction and the shape parameter $\alpha_{JM} = A_J/A_M$ of the adherent cell according to Eq. 17:

$$\frac{\underline{V}_J}{\underline{I}_M} = \frac{r_J}{\eta_J}\frac{A_J}{A_M}. \tag{17}$$

We determined the contact areas A_J of the 12 cells from micrographs and the membrane areas A_M from the capacitance measurements. The shape parameters $\alpha_{JM} = A_J/A_M$ are plotted in Fig. 7 *a* in the order of increasing values. There is a wide variability from, $\alpha_{JM} = 0.2$ indicating a small adhesion contact, to $\alpha_{JM} = 0.5$ for a pancake-shaped cell.

By combining the AC transimpedance $\underline{V}_J/\underline{I}_M$ with the shape parameter A_J/A_M, we evaluated the global conductance $G_J = \eta_J/r_J$ using Eq. 17. The results are shown in Fig. 7 *b* in the order of increasing values. Most conductances are between 0.5 µS and 1.5 µS with one extreme value at 3.3 µS. From independent measurements we know that the

sheet resistance is $r_J = 24 \pm 5\,M\Omega$ for the conditions of this experiment (10). We assign the variability of the global conductance to the geometry parameter η_J. Using $r_J = 24\,M\Omega$, we obtain values in a range between $\eta_J = 12$ and $\eta_J = 35$, as indicated in Fig. 7 *b*. The lowest value is near the minimum $\eta_J = 4\pi$ for local recording in the center of a circular junction. The larger values indicate more peripheral recordings and less compact adhesion areas. The extreme parameter $\eta_J = 80$ refers to a cell with arborized structure where part of the membrane current did not contribute to the recorded voltage.

CONCLUSION

By transistor recording we probed a cell membrane in contact to extracellular matrix protein for the presence and functionality of sodium channels. In the model system of $Na_v1.4$ channels in HEK 293 cells on fibronectin, we found that the density and dynamic properties of Na^+ channels are indistinguishable from the average cell membrane that is probed by whole-cell patch clamp. By achieving a direct coupling of the sodium current in mammalian cells with the electron current in a silicon transistor, we implemented a fundamental element of bioelectronics that is the basis for an optimization of interfacing neuronal systems with semiconductor devices and for a development of cell-based biosensors. A crucial subject of further research is an investigation of induced channel accumulation in the area of cell adhesion by suitable coating of the substrate.

APPENDIX: ONE-COMPARTMENT MODEL

Current conservation in the planar core-coat conductor of a cell-semiconductor junction with Na^+ channels is expressed by Eq. A1 with the voltage profile V_J in the cell-chip junction, the intracellular voltage V_M, and the reversal voltage of sodium V_0^{Na}, at constant voltage of the substrate (7). c_M and c_S are the area-specific capacitances of membrane and substrate, r_J is the sheet resistance of the electrolyte between cell and substrate, and g_{JM}^{Na} is the Na^+ conductance of the attached membrane:

$$(c_M + c_S)\frac{\partial V_J}{\partial t} - \frac{1}{r_J}\nabla^2 V_J = c_M\frac{dV_M}{dt} + g_{JM}^{Na}(V_M - V_0^{Na} - V_J). \tag{A1}$$

Current conservation in a one-compartment model (7,9) is expressed by Eq. A2 per unit area of the junction with a representative voltage V_J and an area-specific conductance g_J of the junction with the bath on ground potential:

$$(c_M + c_S)\frac{dV_J}{dt} + g_J V_J = c_M\frac{dV_M}{dt} + g_{JM}^{Na}(V_M - V_0^{Na} - V_J). \tag{A2}$$

A match of the one-compartment model to the planar core-coat conductor is defined by a substitution $-r_J^{-1}\nabla^2 V_J \Rightarrow g_J V_J$. A suitable substitution depends on the type of experiment to be considered. In this study, we investigate a stationary AC or DC current through the attached cell membrane. For small extracellular voltages V_J, we obtain Eqs. A3 and A4, where j_{JM} is the ionic or capacitive current per unit area:

$$-\frac{1}{r_J}\nabla^2 V_J \approx j_{JM} \tag{A3}$$

$$g_J V_J \approx j_{JM}. \tag{A4}$$

The voltage profile $V_J(a)$ along the radius coordinate a of a circular junction with radius a_J is given by Eq. A5, with a total current $A_J j_{JM}$ through a contact area $A_J = \pi a_J^2$:

$$V_J = A_J j_{JM}\frac{r_J}{4\pi}\left(1 - \frac{a^2}{a_J^2}\right). \tag{A5}$$

Identification $V_J(a)$ in Eq. A5 with the representative voltage V_J in Eq. A4 yields the area-specific conductance g_J of the one-compartment model according to Eq. A6 with a geometry parameter η_J:

$$\frac{1}{g_J} = \frac{A_J r_J}{\eta_J}, \quad \eta_J = \frac{4\pi}{1 - a^2/a_J^2}. \tag{A6}$$

The geometry parameter is $\eta_J = 4\pi$ for local voltage recording in the center of a circular junction and larger for more peripheral recordings. Also for a less compact adhesion area with ellipsoidal or arborized shape, the total current $A_J j_{JM}$ through the attached membrane is less efficient to contribute to the recorded voltage and gives rise to an enhanced geometry parameter η_J.

We thank Günther Zeck and Paolo Bonifazi for the chips, Michaela Morawetz and Ingmar Schoen for support with molecular biology, Matthias Brittinger for advice with transistor recording, and Ingmar Schoen for critical reading of the manuscript.

This project was supported by the Deutsche Forschungsgemeinschaft (SFB 563) and by the European Union (Information Society Technologies Program).

REFERENCES

1. Vassanelli, S., and P. Fromherz. 1999. Transistor probes local potassium conductances in the adhesion region of cultured rat hippocampal neurons. *J. Neurosci.* 19:6767–6773.
2. Straub, B., E. Meyer, and P. Fromherz. 2001. Recombinant maxi-K channels on transistor, a prototype of iono-electronic interfacing. *Nat. Biotechnol.* 19:121–124.
3. Brittinger, M., and P. Fromherz. 2005. Field-effect transistor with recombinant potassium channels: fast and slow response by electrical and chemical interactions. *Appl. Phys. A.* 81:439–447.
4. Trimmer, J. S., S. S. Cooperman, S. A. Tomiko, J. Y. Zhou, S. M. Crean, M. B. Boyle, R. G. Kallen, Z. H. Sheng, R. L. Barchi, F. J. Sigworth, R. H. Goodman, W. S. Agnew, and G. Mandel. 1989. Primary structure and functional expression of a mammalian skeletal-muscle sodium channel. *Neuron.* 3:33–49.
5. Chen, H. J., D. Gordon, and S. H. Heinemann. 2000. Modulation of cloned skeletal-muscle sodium channels by the scorpion toxins LqhII, LqHIII, and Lqh alphaIT. *Pflugers Arch.* 439:423–432.
6. Weis, R., B. Müller, and P. Fromherz. 1996. Neuron adhesion on silicon chip probed by an array of field-effect transistors. *Phys. Rev. Lett.* 76:327–330.
7. Weis, R., and P. Fromherz. 1997. Frequency dependent signal transfer in neuron transistors. *Phys. Rev. E.* 55:877–889.
8. Giaever, I., and C. R. Keese. 1991. Micromotion of mammalian cells measured electrically. *Proc. Natl. Acad. Sci. USA.* 88:7896–7900.
9. Regehr, W. G., J. Pine, C. S. Cohan, M. D. Mischke, and D. W. Tank. 1989. Sealing cultured invertebrate neurons to embedded dish electrodes facilitates long-term stimulation and recording. *J. Neurosci. Methods.* 30:91–106.
10. Gleixner, R. J., and P. Fromherz. 2003. Contact resistance of cell-silicon junctions measured with voltage-sensitive dye. *Biophys. J.* 84:584A–585A.